2012

Experimental and Theoretical Study on Condensation Heat Transfer of Nonazeotropic Refrigerant Mixtures R1234yf/R32 Inside a Horizontal Smooth Tube

Linlin Wang
wanglinlin@hee.k.u-tokyo.ac.jp

Chaobin Dang

Eiji Hihara

Experimental and Theoretical Study on Condensation Heat Transfer of Nonazeotropic Refrigerant Mixture R1234yf/R32 inside a Horizontal Smooth Tube

Linlin Wang*, Chaobin Dang, Eiji Hihara

Institute of Environmental Studies, Graduate School of Frontier Sciences, The University of Tokyo, 5-1-5 Kashiwanoha, Kashiwa-shi, Chiba 277-8563, Japan

*Corresponding author. E-mail: [wanglinlin@hee.k.u-tokyo.ac.jp] Tel./Fax: [+81 4 7136 4631]
Postal address: Environmental Studies Building #285, the University of Tokyo, 5-1-5 Kashiwanoha, Kashiwa, Chiba 277-8563, Japan

ABSTRACT

The condensation heat transfer characteristics of nonazeotropic mixtures R1234yf and R32 (mass fractions of 0.52:0.48 and 0.77:0.23, respectively) inside a horizontal smooth tube (inner diameter 4 mm) were experimentally studied at mass fluxes ranging from 100 to 300 kg/m^2 s. A prediction model for the forced convective condensation heat transfer characteristics of nonazeotropic refrigerant mixtures was also constructed based on the measured results, and the details are presented. The heat transfer characteristics, especially the heat transfer deterioration of the nonazeotropic refrigerant mixture, are evaluated by combining the correlations of heat transfer and mass transfer at both the vapor side and liquid side. By comparison with experimental data, prediction results obtained using the proposed model were found to agree reasonably with the experimental condensation heat transfer coefficient of binary refrigerant mixtures using R1234yf and R32.

1. INTRODUCTION

Increasing concerns regarding the environment have resulted in the evolution of refrigerants from chlorofluorocarbons and hydrochlorofluorocarbons to hydrofluorocarbons(HFCs) in developed countries. Although HFC refrigerants have no ozone depletion potential, many of them have a relatively high global warming potential (GWP). For example, R134a, having a GWP of 1300, is used extensively in automobile air conditioners. R1234yf was jointly developed by Honeywell and DuPont to be a promising candidate for use in mobile air conditioners owing to its low GWP of 4 and thermophysical properties similar to those of R134a. The condensation heat transfer performance of R1234yf and the effects of various parameters on heat transfer characteristics have been experimentally investigated (Wang et al., 2012). Increasing concerns regarding the environmental impact of HFCs used in residential air conditioners have also led to the reconsideration of refrigerants in these applications. R1234yf cannot be used as an alternative to R410a because it operates at lower pressures and has smaller latent heat. One approach to balance both the environmental and performance requirements is to use a refrigerant mixture of R1234yf and R32 to obtain a high system coefficient of performance. The thermophysical properties of refrigerant mixtures are also being evaluated (Arakawa et al., 2010), in addition to the flow boiling heat transfer characteristics of both pure R1234yf (Saitoh et al., 2011) and a refrigerant mixture of R1234yf/R32 (Li et al., 2012). However, only limited information is available regarding the condensation of a refrigerant mixture of R1234yf/R32.

Some theoretical studies have predicted the local heat and mass transfer characteristics of refrigerant mixtures during condensation. Koyama et al. (1998) developed a method of predicting the condensation characteristics of binary refrigerant mixtures in a horizontal tube based on the assumption that the phase equilibrium is established at the vapor-liquid interface. In this model, it was assumed that the radial distribution of the mass fraction in a liquid film is uniform and that the mass transfer coefficient is infinitely large. Furthermore, they compared the predicted results with the experimental data obtained for the condensation of R134a/R123 mixtures. Jin et al. (2003) established a model of condensation of binary nonazeotropic refrigerant mixtures in a horizontal smooth tube by considering both the liquid-side and vapor-side mass transfers. To verify the validity of the model, they compared the predicted results with the experimental data of Koyama using R134a/R123 mixtures (Koyama et al., 1998).

In this study, the condensation heat transfer characteristics of nonazeotropic mixtures R1234yf and R32 inside a horizontal smooth tube (inner diameter 4 mm) were experimentally studied. The measured local heat transfer coefficients were evaluated by a prediction model for the forced convective condensation heat transfer characteristics of nonazeotropic refrigerant mixtures to predict the heat transfer deterioration by taking into consideration the mass transfers at both the vapor side and liquid side.

2. EXPERIMENTAL APPARATUS

Figure 1 shows a schematic of the experimental apparatus. The refrigerant loop comprises a test section, two sight glasses, a post-condenser, an accumulator, an expansion valve, a filter, a liquid pump, a mass flow meter, an evaporator, and three water baths. The saturation temperature and pressure of the test section are controlled by the opening of the expansion valve, and the water baths are used to adjust the inlet superheating of the test section, provide cooling water to the test section, and subcool the refrigerant flowing out of the test section.

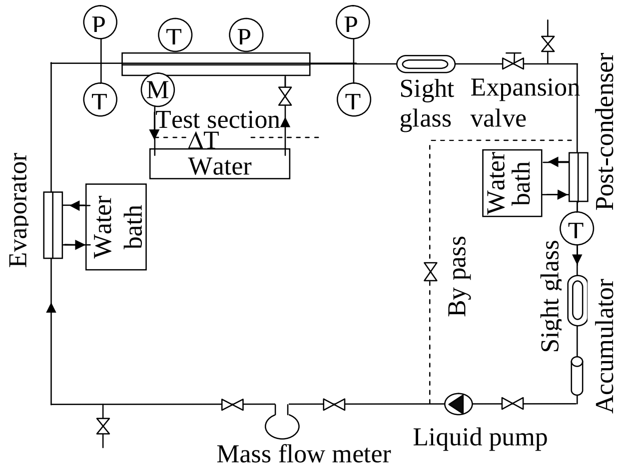

Figure 1: Schematic of the experimental apparatus

Figure 2 shows a detailed diagram of the test sub-sections. The test condensation tube is made of copper with an inner diameter of 4 mm and an overall length of 3.4 m. It is divided into five sub-sections with each sub-section having an effective length of 0.45 m. All of the sub-sections were cooled separately by the cooling water, and the average condensation heat transfer coefficient of each sub-section was measured. The refrigerant flows inside the copper tube, and the cooling water flows in the reverse direction within the annular region between the inner tube and outer tube.

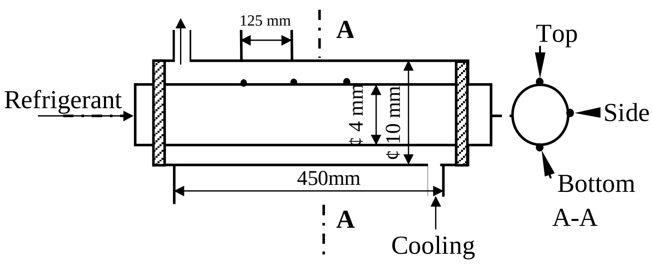

Figure 2: Detailed diagram of a test sub-section

For each sub-section, the mass flow rate of the cooling water was controlled independently. In order to make the average heat flux in each sub-section almost the same, the inlet temperature and mass flow rate of the cooling water were controlled. The inlet and outlet temperatures of the cooling water were measured using platinum resistance sensors. Nine T-type thermocouples were soldered on the outer surface of the copper tube with an interval of 12.5 cm between thermocouples. To reduce the heat loss to the surroundings, the entire apparatus including the refrigerant loop and the coolant loop was well insulated.

The cooling water loop includes a re-circulating chiller, mass flow meters, filters, and flow rate controlling valves. The re-circulating chiller provides cooling water for each sub-section at the desired temperature. The temperatures at the inlet and outlet of each sub-section were measured using platinum resistance sensors. The cooling water flow rate of each sub-section was measured using a positive displacement flow meter attached to the respective path.

All the temperature sensors, including the thermocouples and platinum resistance sensors, were calibrated using a high precision resistance thermometer (Chino, Model F201-A-2) with an accuracy of ±0.01°C. The accuracy of the calibrated thermocouples was within ±0.1°C, and that of the calibrated platinum resistance sensors was within ±0.05°C. The mass flow rate on the refrigerant side was measured by a Coriolis-type mass flow meter with an accuracy of ±0.1%. The mass flow rates of the cooling water were measured by positive displacement flow meters with an accuracy of ±1.0%. Changes in pressure inside the test section were measured using an ultra precision Digiquartz manometer (Sokken, Model 660) with an accuracy of ±1.0 kPa. The flow patterns inside the sight glass were observed and recorded using a high-speed digital camera (Photron, FASTCAM SA4). The accuracy of the length of the test sections was within ±1.0 mm, and the diameter of the tube was within ±0.1 mm.

3. PREDICTION MODEL

3.1 Physical Model

Figure 3 shows the physical model employed in the prediction method. The following assumptions were made in this model similar to Jin et al. (2003). (1) The phase equilibrium is established at the vapor-liquid interface; i.e., the bulk vapor is in a saturated state and the bulk liquid is subcooled, as shown in Figure 4. (2) The frictional pressure drop behavior is the same as that of the condensation for a pure refrigerant and estimated by the correlation of Haraguchi et al. (1994). (3) The heat transfer coefficient of a liquid film is estimated by the correlation of Haraguchi et al. (1994) developed for the condensation of a pure refrigerant. (4) The flow is annular with uniform film thickness along the tube circumference. (5) The convective heat transfer in the vapor phase is negligible.

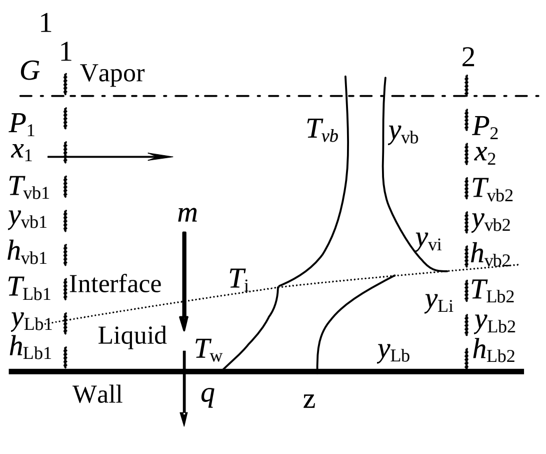

Figure 3: Physical model

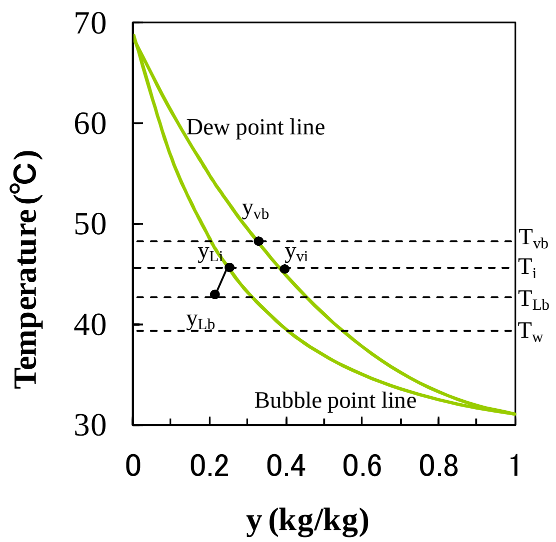

Figure 4: Phase equilibrium diagram

3.2 Calculation Models

The local condensation heat transfer coefficient was determined by calculating the ratio of the average heat flux q_w to the temperature difference between the thermodynamic equilibrium temperature of refrigerant T_b and the inner wall temperature T_w,

$$h = \frac{q_w}{T_b - T_w} \tag{1}$$

The pressure drop is calculated using the correlation of Haraguchi et al. (1994) for the frictional pressure drop added to the acceleration pressure drop, given in equations (2) and (3), where the two-phase multiplier and void fraction are shown in equations (4) and (5), respectively.

$$\left(-\frac{\mathrm{dP}}{\mathrm{dz}}\right) = -G^2 \frac{d}{dz}\left[\frac{x^2}{\alpha\rho_v} + \frac{(1-x)^2}{(1-\alpha)\rho_L}\right] + \left(-\frac{\mathrm{dP}}{\mathrm{dz}}\right)_f \tag{2}$$

$$\left(-\frac{\mathrm{dP}}{\mathrm{dz}}\right)_f = \Phi_V^2 \frac{0.092 G^2 x^2}{\rho_v d \,\mathrm{Re}_v^{0.2}} \tag{3}$$

$$\Phi_V = 1 + 0.5\left[\frac{G}{\sqrt{g d \rho_g\left(\rho_l - \rho_g\right)}}\right]^{0.75} X_{tt}^{\,0.35} \tag{4}$$

$$\alpha = \left[1 + \frac{\rho_v}{\rho_l}\left(\frac{1-x}{x}\right)\left(0.4 + 0.6\sqrt{\frac{\frac{\rho_l}{\rho_v} + 0.4\left(\frac{1-x}{x}\right)}{1 + 0.4\left(\frac{1-x}{x}\right)}}\right)\right]^{-1} \tag{5}$$

For the heat balance of the refrigerant, the inside wall heat flux is shown in equation (6). The convective condensation heat transfer coefficient h_o at interface of pure refrigernat is calculated using the correlation of Haraguchi et al. (1994) where the properties are based on the mass fraction and temperature of the reference bulk liquid film.

$$q_w = h_o\left(T_i - T_w\right) = -\frac{G}{\pi d}\frac{d}{dz}\left(x h_{vb} + \left(1-x\right) h_{lb}\right) \tag{6}$$

The mass balance equations of the more volatile component of both the vapor and liquid sides are shown in equations (7) and (8), and the mass transfer coefficients of the vapor and liquid sides are estimated by the correlations of Koyama et al. (1998) and Lamourelle et al. (1972), respectively, as shown in equations (9)–(11).

$$m_A = -\frac{G}{\pi d}\frac{d(x y_{vb})}{dz} = -\frac{G y_{vi}}{\pi d}\frac{dx}{dz} - k_v (y_{vi} - y_{vb}) \tag{7}$$

$$m_A = \frac{G}{\pi d}\frac{d((1-x) y_{lb})}{dz} = -\frac{G y_{li}}{\pi d}\frac{dx}{dz} + k_l (y_{li} - y_{lb}) \tag{8}$$

$$k_V = \frac{\rho_V D_V}{d} Sh_V = \frac{\rho_V D_V}{d} 0.023\sqrt{\alpha}\,\Phi_v^2\,\mathrm{Re}_v^{0.8}\, Sc_v^{0.3} \tag{9}$$

$$k_L = \frac{\rho_L D_L}{\delta_L} Sh_L = \frac{\rho_V D_V}{\delta_L}(1.76\times 10^{-5})\,\mathrm{Re}_L^{1.506}\, Sc_L^{0.5} \tag{10}$$

$$\delta_L = (1-\sqrt{\alpha}) d / 2 \tag{11}$$

The temperature of the reference bulk liquid film is calculated using equation (12).

$$T_{Lb} = T_w + \frac{2}{3}(T_i - T_w) \tag{12}$$

3.3 Calculation Procedure

Considering a control volume between z and z+Δz during condensation, the heat and mass transfer equations derived are solved numerically under the conditions that the heat flux, mass flux, and thermodynamic state of refrigerant at the inlet are specified as known parameters. In addition, the inlet refrigerant is set as a saturated state. The calculation procedure is described as follows:

(1) Calculate the refrigerant conditions at the inlet, and specify the control volume length Δz.
(2) The vapor quality at the outlet is calculated by thermodynamic state equations.
(3) Assume the mass fraction of both the vapor and liquid at the outlet, and estimate the bulk mass fraction of the vapor and liquid.
(4) Calculate the pressure drop from equations (2)–(5), and the refrigerant conditions at the outlet.
(5) Assume the wall temperature, and calculate h_L by the correlation of Haraguchi et al. (1994).
(6) Assume $\Delta z = \Delta z_{vm}$, and calculate y_{vi} by mass transfer balance equations (7) and (9). Then, determine y_{Li} and T_i from thermodynamic state equations
(7) Calculate the wall temperature from equation (6) and return to Step (5) until it equals to the assumed wall temperature.
(8) Calculate the reference bulk liquid temperature by equation (12).
(9) Determine Δz_{Lm} from the mass transfer balance equations (8)–(11).
(10) Calculate Δz_H from equation (6).
(11) Steps (3)–(9) are repeated until the following equation is satisfied: $\Delta z = \Delta z_H = \Delta z_{Lm}$.
(12) Continue the above procedure until x = 0.

4. RESULTS AND DISCUSSION

4.1 Comparison of heat transfer characteristics between prediction and experiment

Figure 5 shows the comparison of the measured and predicted heat transfer coefficients of R1234yf and R32 against the vapor quality at two mass fractions of 0.77:0.23 and 0.52:0.48. Owing to the influence of mass transfer at the heat transfer interface, the heat transfer coefficient decreases rapidly with the decrease in vapor quality. Comparison of results show that the prediction model can fit the tendency of the experimental results, in which the heat transfer coefficient decreases with a decrease in vapor quality and mass flux. The deviation of predicted values and experimental results at a mass flux of 100 kg/m^2 s is relatively large compared with that at the other two mass fluxes.

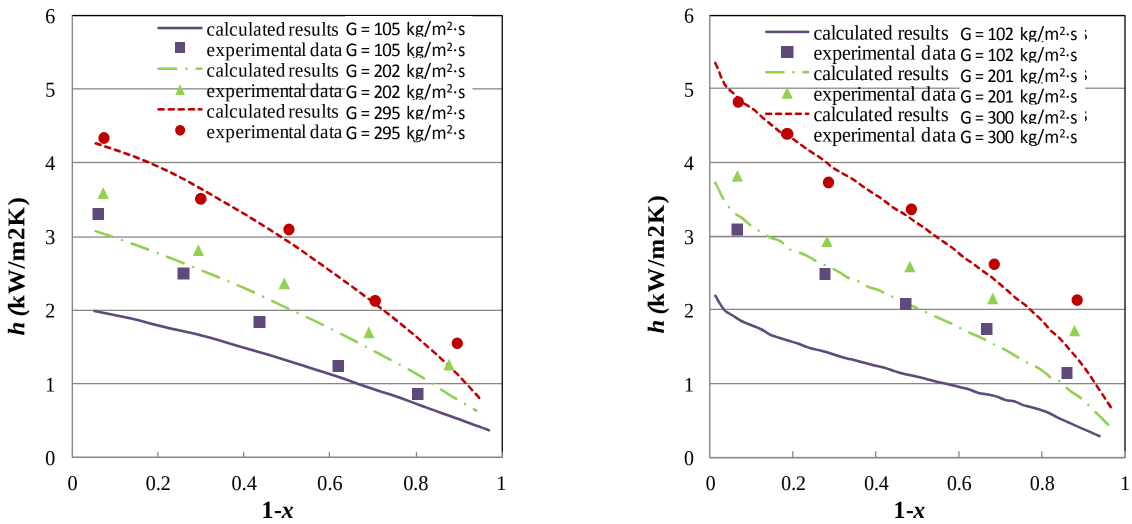

Figure 5: Comparison between the measured and predicted heat transfer coefficients of R1234yf/R32(mass fraction 0.77:0.23and 0.52:0.48) at different mass fluxes.

In addition, the deviation at a mass fraction of 0.52:0.48 is higher than that at a mass fraction of 0.77:0.23, with a mean value of all data approximately 23%. Therefore, more work should be done to decrease the experimental measurement error and enhance the applicability of the physical model at small mass fluxes.

4.2 Heat transfer deterioration of the nonazeotropic refrigerant mixtures

The temperature glide at a mass fraction of 0.77:0.23 is about 6.5°C, while that at a mass fraction of 0.52:0.48 is about 4.1°C. Here, the heat transfer deterioration of the nonazeotropic refrigerant mixtures R1234yf/R32 at mass fraction of 0.77:0.23 was analyzed because it has the highest temperature glide. Figure 6 displays the distribution of calculated vapor bulk temperature, interface temperature, reference bulk liquid temperature, and inner wall temperature compared with experimental bulk temperature and inner wall temperature against axial position along the condenser of R1234yf/R32 (mass fraction 0.77:0.23) at a mass flux of 300 kg/m^2·s. The interface temperature is lower than the vapor bulk temperature owing to the influence of mass transfer at both the vapor and liquid sides at the heat transfer interface, with the largest difference of 0.3°C. It also shows that the predicted vapor bulk temperature and inner wall temperatures agree well with the measured values.

Considering the influence of mass transfer of both vapor and liquid sides in heat transfer, Figure 7 depicts the heat transfer coefficient of R1234yf/R32 (0.77:0.23) at a mass flux of 300 kg/m^2·s when considering mass transfer at both sides, only the vapor side mass transfer, only the liquid side mass transfer, and without mass transfer. The temperature glide is primarily caused by the mass transfer of the vapor side, which attributed the most to the decrease of the interface temperature lower than the vapor bulk temperature.

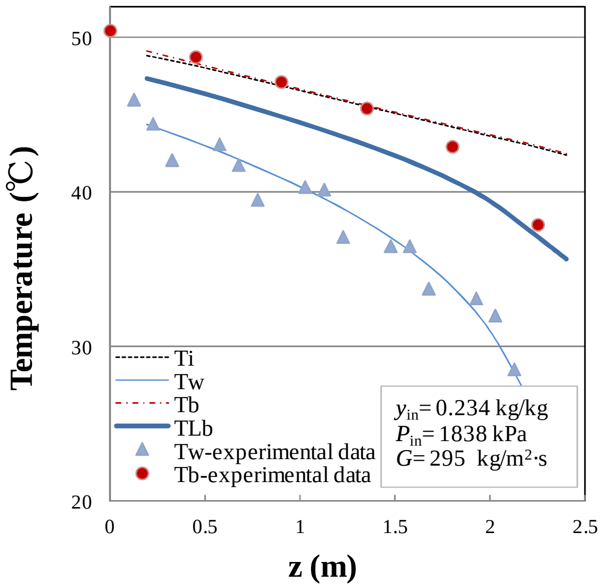

Figure.6: Temperature distribution along the tube of R1234yf/R32 (0.77:0.23) at mass flux of 300 kg/m^{2}s.

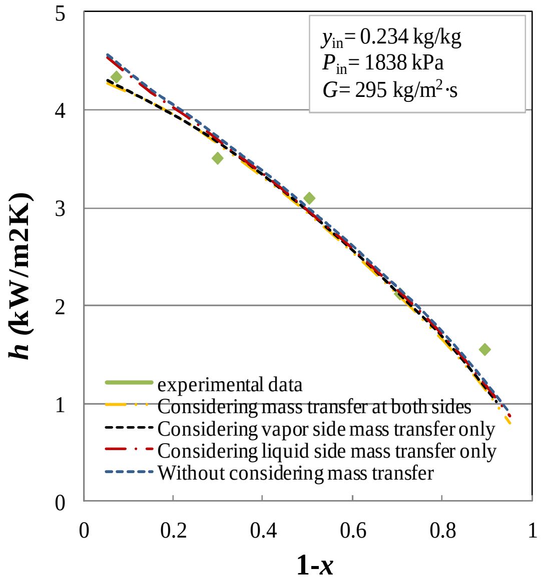

Figure.7: Heat transfer coefficient of R1234yf/R32 (0.77:0.23) at a mass flux of 300 kg/m^2·s.

5. CONCLUSIONS

Condensation heat transfer characteristics of nonazeotropic mixtures R1234yf and R32 (mass fractions og 0.52:0.48 and 0.77:0.23, respectively) inside a horizontal smooth tube were experimentally studied. The heat transfer characteristics, especially the heat transfer deterioration of the nonazeotropic refrigerant mixture were evaluated by combining the correlations of the heat transfer and mass transfer at both the vapor side and liquid side. The main conclusions are as follows:

- The proposed model can predict the saturated temperature and wall temperature well, and the difference between the saturated temperature and the interface temperature is small when using R1234yf and R32 even at a mass fraction of 0.77:0.23.
- The calculated results show that the main mass transfer resistance is at the vapor side, while the mass transfer resistance at the liquid film has relatively less influence on the heat transfer coefficient compared to the vapor side.
- Prediction results obtained using the proposed model are found to agree reasonably with the experimental heat transfer coefficient when using nonazeotropic mixtures of R1234yf and R32, the mean deviation of the predicted and experimental data is about 23%.
- The deviation of the predicted value and experimental results at a mass flux of 100 kg/m^2·s is relatively large compared with that at the other two mass fluxes. Further study should be conducted to decrease the experimental measurement error and enhance the applicability of the physical model at small mass fluxes.

NOMENCLATURE

d	inner diameter	(m)
h	heat transfer coefficient	(kW/m^2·K)
G	mass flux	(kg/m^2·s)
k	mass transfer coefficient	(kg/m^2·s)
m	condensation mass flux	(kg/m^2·s)
P	pressure	(Pa)
q	heat flux	(kW/m^2)
T	temperature	(°C)
x	vapor quality	(kg/kg)
y	mass fraction of R32	(kg/kg)
z	axial position	(m)
Re	Reynolds number	
Greek symbols		
α	void fraction	
λ	thermal conductivity	(W m^{-1} K^{-1})
μ	viscosity	(Pa·s)
ρ	density	(kg m^{-3})
σ	surface tension	(N m^{-1})
Φ_V	two-phase flow multiplier for frictional pressure drop	

Subscripts

1	cross section 1
2	cross section 2
A	more volatile component
b	bulk
i	vapor-liquid interface
in	inlet
l	liquid
v	vapor
w	wall

REFERENCES

Arakawa, Y., Kim, S., Kamiaka, T., Dang, C., Hihara, E., 2010, Thermal property measurement of HFO-1234yf + HFC-32 mixture, *International Symposium on Next generation Air Conditioning and Refrigeration Technology*, Feb.17-19, Tokyo, Japan. NS22.

Fujii, T., 2005, Film Condensation Heat Transfer, Chapter 7, *Kyushu University Press*, Fukuoka, Japan: p. 177-213.

Haraguchi, H., Koyama, S., Fujii, T., 1994, Condensation of refrigerants HCFC22, HFC 134a and HCFC123 in a horizontal smooth tube, *Transactions of the Japan Society of Mechanical Engineers.*, vol. 60, no. 574: p. 2117-2124.

Jin, D. X., Kwon, J. T., Kim, M. H., 2003, Prediction of in-tube condensation heat transfer characteristics of binary refrigerant mixtures, *International Journal of Refrigeration*, vol. 23: p. 593-600.

Koyama, S., Yu, J., ISHIBASHI, A., 1998, Condensation of binary refrigerant mixtures in a horizontal smooth tube, *Thermal Science & Engineering.*, vol. 6, no. 1: p. 123-129.

Lamourelle, A. P., Sandall, O. C., 1972, Gas absorption into a turbulent liquid, *Chemical Engineering Science.*, vol. 27, no. 10: p. 35-43.

Li, M. X., Dang, C. B., Hihara, E., 2012, Flow boiling heat transfer of HFO1234yf and R32 refrigerant mixtures in a smooth horizontal tube: Part I. Experimental investigation, *International Journal of Heat and Mass Transfer*, vol. 55: p. 3437-3746.

Poling, B. E., Prausnitz, J. M., O'Connell, J. P., 2000, The Properties of Gases and Liquids, Chapter 11, Fifth Edition, McGRAW-HILL.

Saitoh, S., Dang, C. B., Nakamurab, Y., Hihara, Eiji., 2011, Boiling heat transfer of HFO-1234yf flowing in a smooth small-diameter horizontal tube, *International Journal of Refrigeration*., vol. 34: p. 1846-1853.

Wang, L. L., Dang, C. B., Hihara, E., 2012, Experimental study on condensation heat transfer and pressure drop of low GWP refrigerant HFO1234yf in a horizontal tube, *International Journal of Refrigeration*, (in press).

ACKNOWLEDGEMENT

This study was sponsored by the "Development of Non-fluorinated Energy-Saving Refrigeration and Air Conditioning Systems" project of the New Energy and Industrial Technology Development Organization of Japan. The authors would like to thank Daikin Industries, Ldt for provide the refrigerant HFO1234yf.